Hindawi Publishing Corporation
International Journal of Photoenergy
Volume 2013, Article ID 765938, 8 pages
http://dx.doi.org/10.1155/2013/765938

Research Article

Interface Study of ITO/ZnO and ITO/SnO_2 Complex Transparent Conductive Layers and Their Effect on CdTe Solar Cells

Tingliang Liu, Xing Zhang, Jingquan Zhang, Wenwu Wang, Lianghuan Feng, Lili Wu, Wei Li, Guanggen Zeng, and Bing Li

College of Materials Science and Engineering, Sichuan University, Chengdu 610064, China

Correspondence should be addressed to Guanggen Zeng; yigezeng@sina.com

Received 28 September 2012; Accepted 18 December 2012

Academic Editor: Sudhakar Shet

Transparent ITO/ZnO and ITO/SnO_2 complex conductive layers were prepared by DC- and RF-magnetron sputtering. Their structure and optical and electronic performances were studied by XRD, UV/Vis Spectroscopy, and four-probe technology. The interface characteristic and band offset of the ITO/ZnO, ITO/SnO_2, and ITO/CdS were investigated by Ultraviolet Photoelectron Spectroscopy (UPS) and X-ray Photoelectron Spectroscopy (XPS), and the energy band diagrams have also been determined. The results show that ITO/ZnO and ITO/SnO_2 films have good optical and electrical properties. The energy barrier those at the interface of ITO/ZnO and ITO/SnO_2 layers are almost 0.4 and 0.44 eV, which are lower than in ITO/CdS heterojunctions (0.9 eV), which is beneficial for the transfer and collection of electrons in CdTe solar cells and reduces the minority carrier recombination at the interface, compared to CdS/ITO. The effects of their use in CdTe solar cells were studied by AMPS-1D software simulation using experiment values obtained from ZnO, ITO, and SnO_2. From the simulation, we confirmed the increase of E_{ff}, FF, V_{oc}, and I_{sc} by the introduction of ITO/ZnO and ITO/SnO_2 layers in CdTe solar cells.

1. Introduction

Transparent conducting oxide (TCO) layers have been extensively studied because of their use as transparent electrodes in displays and in photovoltaic devices [1]. By incorporating a high resistance layer, the thickness of a conducting cadmium sulfide (CdS) layer can be reduced, which significantly improves the blue response of CdTe devices [2] and makes CdTe thin-film solar cells more competitive [3]. Wu has reported the efficiency of 16.5% with <100 nm CdS thickness [4]. However, as the thickness of CdS is decreased, the films would become discontinuous leading to the formation of localized CdTe/TCO junction, which leads to excessive shunting and therefore lowers the solar cell efficiency [5]. Using complex transparent conductive layers is known as a feasible method to improve the characteristics of CdTe thin films solar cells. Indium-tin oxide (ITO) systems, SnO_2, and ZnO have been used as the high resistance layer because of their excellent electrical and optical properties [6, 7] and the improvement of device performance [8].

The complex transparent conductive layers are always heterojunction structure, which are rather complicated systems for their different electron affinities, band gaps. The band offset and interface properties of a heterostructure are some of the most important properties. Sheng et al. have studied the n-layer/transparent conducting oxide (n/TCO) interfaces in amorphous silicon (a-Si:H) and microcrystalline silicon (mc-Si:H) materials by XPS [9]. Liu et al. studied the interface properties and band alignment of Cu_2S/CdS heterojunction, and the band offsets are obtained [10]. Horn studied electronic structure at the interface, relating to band bending and the evolution of transport barriers such as the Schottky barrier and the heterojunction band offset [11]. Bernède and Marsillac. have measured the band offsets of SnO_2/γ-In_2Se_3 heterojunction by XPS and estimated the conduction band discontinuity ΔE_c to be -0.3 ± 0.3 eV [12]. Mönch discussed the electronic properties and chemical interactions at GaAs (110) and InP (110) surfaces [13].

In this present work, ITO, ZnO, and SnO_2 films have been successfully prepared on ITO coated glass substrate by DC- and RF-magnetron sputtering and characterized by XRD, UV/Vis spectra, and four-probe apparatus. UPS and XPS were used to characterize the band offset of ITO/CdS,

Table 1: The parameters used in the AMPS-1D simulation.

	ITO	ZnO	SnO_2	CdS	CdTe
Eg (eV)	3.72	3.27	4.11	2.42	1.46
EPS	9.4	9	9	9	9.4
Electron mobility ($cm^2/V/s$)	30	100	3.6	340	500
Hole mobility ($cm^2/V/s$)	5	25	1	50	60
Carrier density (cm^{-3})	$4.3 * 10^{20}$	10^{19}	$2.4 * 10^{18}$	10^{17}	$2 * 10^{15}$
Density of state, CB (cm^{-3})	$4 * 10^{19}$	$1.8 * 10^{19}$	$1.8 * 10^{19}$	$1.8 * 10^{19}$	$7.5 * 10^{17}$
Density of state, VB (cm^{-3})	10^{18}	$2.4 * 10^{18}$	$2.4 * 10^{18}$	$2.4 * 10^{18}$	$1.8 * 10^{18}$
Electron affinity	3.6	4	3.44	4.5	4.28
Thickness (μm)	0.4	0.15	0.15	0.15	6

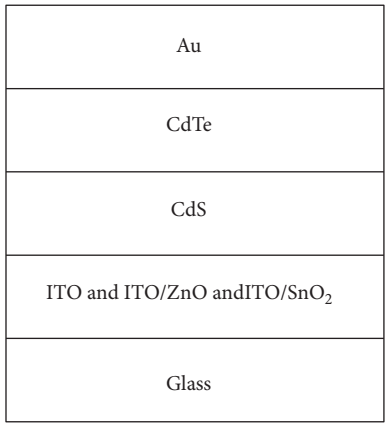

Figure 1: Structural view of CdTe solar cells with different configuration.

ITO/ZnO, and ITO/SnO_2 layers and the influence on the transfer of electrons in CdTe thin film solar cells. AMPS-1D simulations, based on the Poisson equation and the hole-electron continuity equations in one dimension [14], were used to study the device performance of the CdTe solar cells with these different transparent conductive layers.

2. Experiment

DC magnetron was used to sputter the ITO and ZnO films in this paper. The targets were ceramic ITO ($In_2O_3 : Sn_2O_3$ = 90 : 10) and metallic Zn (99.999%).The substrate was held at 300°C while the sputtering pressure was 1.0 Pa for ITO and 2.4 Pa for Zn, of high purity argon (99.999%) mixed with 10% oxygen. The SnO_2 films were prepared on an ITO substrate by RF-magnetron sputtering. Sputtering was conducted at 267°C and 1.0 Pa of argon (99.999%) mixed with 1% oxygen. The ITO layers were about 400 nm and the ZnO (SnO_2) were about 150 nm. The CdS layers were deposited by chemical bath deposition (CBD) and were about 150 nm thick.

The TCO/CdS structure was analyzed by X-ray diffraction (DX-2500, Dandong Fangyuan Instrument LLC) using Cu Ka radiation (λ = 0.15405 nm). The sheet resistance was measured with a Digital Four-Probe Tester (SZT-2, Suzhou Tongchuan Electronics). The thickness of each film was measured with a stylus profiler (XP-2, Ambios Technology Inc.). The optical transmission was measured by UV/Vis spectrometer (Perkin Elmer Inc., Lambda-950). The XPS and UPS were measured by the multifunctional X-ray Photoelectron Spectroscopy (AXIS Ultra^{DLD}, Kratos Analytical Inc.) with the base pressure ~5.0 $\times 10^{-9}$ Torr, the X-ray of Al K_α, and the X-ray tube power of 130 W. The samples were etched by 21.2 eV He^+ beam and were biased with 7.36 volts to obtain reproducible cut-off results. The work functions were determined from the low-kinetic energy cut-off in the UPS spectra; that is, the intersection of the linear extrapolation with the baseline. In this experiment, samples were cleaned and thinned by sputtering with He^+ ions in HUV.

AMPS-1D has been employed to model and analyze the CdTe solar cells, and the different cells configuration is shown in Figure 1. The parameters used in the simulation are shown in Table 1. The electron affinity energies and mobility were obtained from [15–17]. The thickness of CdTe film was set as 6 μm.

3. Results and Discussion

3.1. XRD. Figure 2 shows XRD patterns of ZnO and SnO_2 films deposited on ITO films. The main diffraction peaks (400), (440), and (222) and so on come from the ITO films. Only one weak peak of ZnO was observed in the spectra labeled as (101), and one weak peak of SnO_2 was observed labeled as (200) at 36.10° diffraction angle. This indicates that the ZnO and SnO_2 films have been deposited successfully onto the ITO films.

3.2. Transmittance. The optical and electrical properties of ITO, ITO/ZnO, and ITO/SnO_2 films were measured. The thickness was 400 nm for ITO films and 150 nm for ZnO and SnO_2 films. Figure 3 shows the optical transmission of the as-deposited ITO/ZnO and ITO/SnO_2 films. At the wavelength from 500 nm to 850 nm, the average transmittance is 82% for ITO/ZnO and 81.64% for ITO/SnO_2 films, respectively, which are not lower than ITO films (85%) too much. On the other hand, in the blue region, the red shifts of the effective absorption edge of ITO/ZnO and ITO/SnO_2 films are clearly observable. The sheet resistance of the ZnO was obtained as 108 Ω/□ while 104 Ω/□ for the SnO_2 films, which are higher than ITO (13.2 Ω/□). The deposition of ZnO or SnO_2 films as high resistance transparent (HRT) on ITO

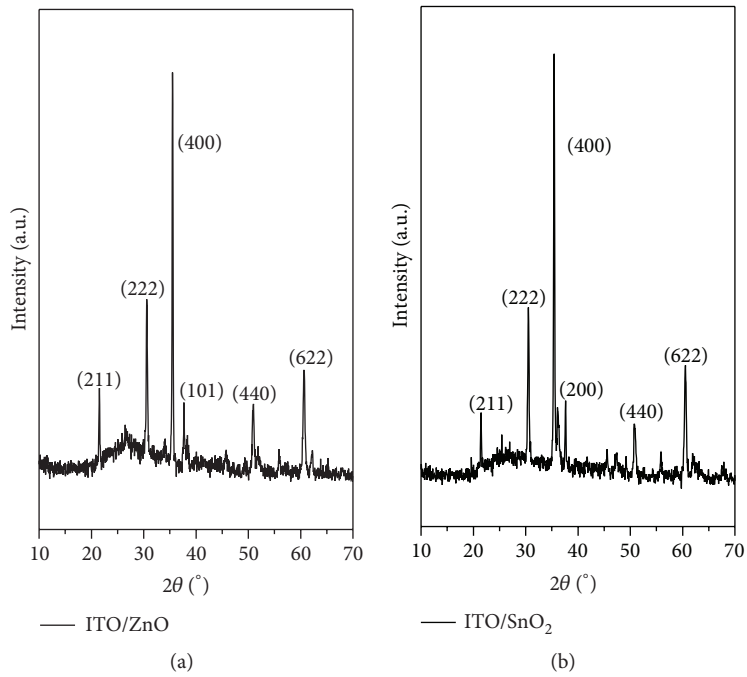

Figure 2: XRD spectrum of ITO/ZnO and ITO/SnO_2 films.

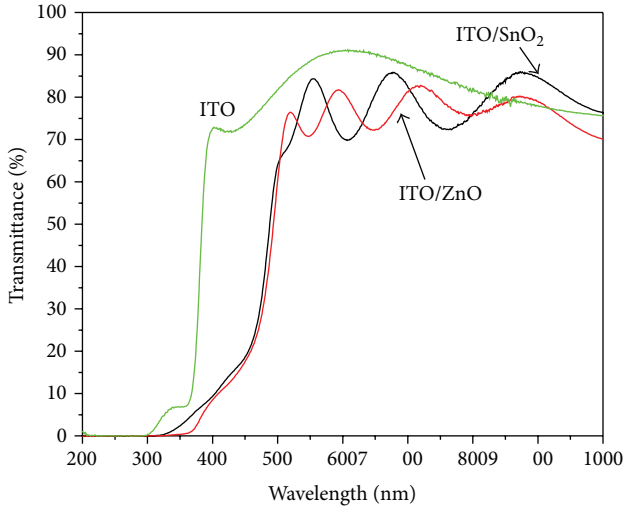

Figure 3: Transmittance spectra of the ITO, ITO/ZnO, and ITO/SnO_2 films.

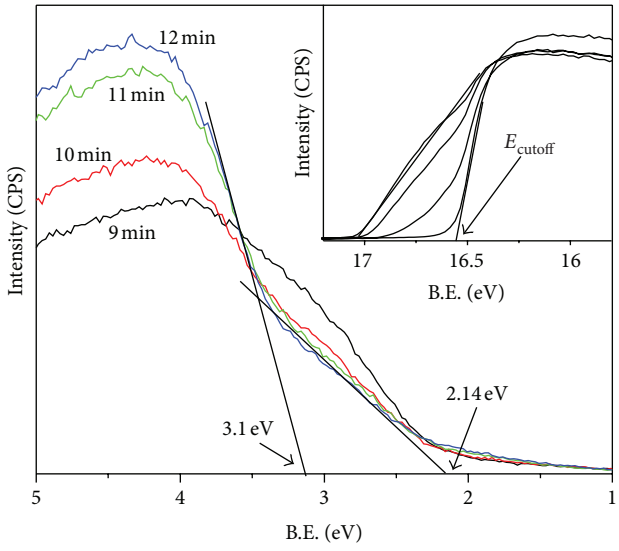

Figure 4: UPS profiling spectra of ITO/CdS films.

films can passivate the CdS surface than ITO, which could eliminate the leakage current caused by the pinhole effects of CdS [15] and thus improves the short circuit current remarkably.

3.3. XPS/UPS. Before analysis with XPS/UPS, all of the samples were cleaned by sputtering with He^+ ions for 1 minute in HUV to eliminate surface effects. The layers were profiled using XPS and UPS by taking spectra after every profiling time intervals until it revealed to the ITO film by He^+ sputtering.

3.3.1. ITO/CdS System. Figure 4 shows the UPS of ITO/CdS structure at different times (9–12 min). The "valence band offset" corresponds to be ($E_F - E_{VBM}$) and provides a direct measure of the Fermi level at the sample surface. The results show that the valence band maximum (VBM) in the interface of ITO/CdS films increases from 2.14 eV to 3.10 eV. The E_{cutoff} (secondary electron onset) is the abscissa value on the left side when the intensity is 0 in the later UPS, so the work function can be obtained by

$$\Phi = h\nu - \left(E_{cutoff} - E_{Fermi}\right). \quad (1)$$

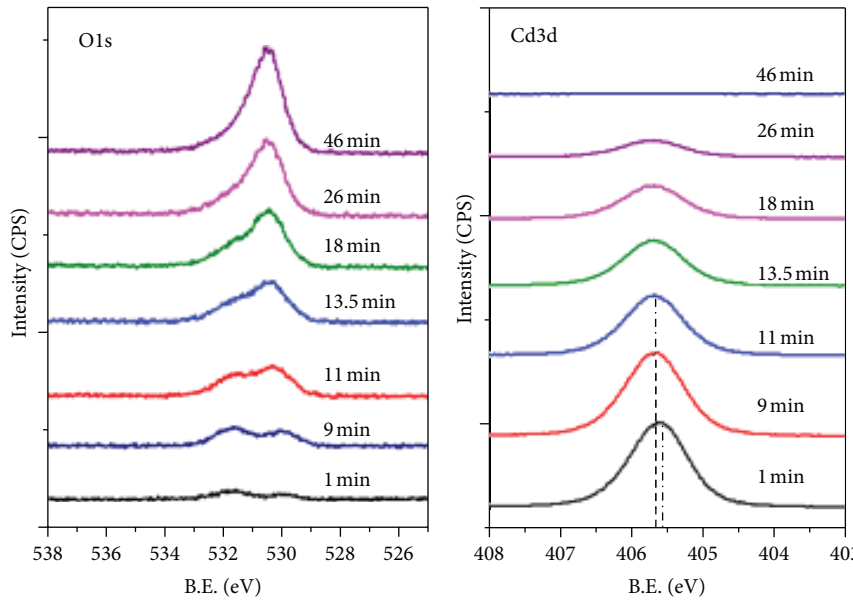

Figure 5: XPS spectrum of the O1s and Cd3d reigns for n-ITO/n-CdS isotype heterojunction at various profiling times.

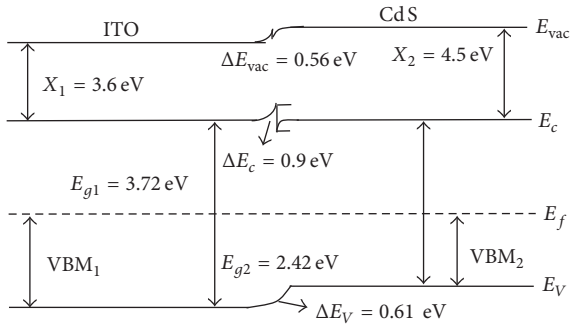

Figure 6: Energy band diagram of the ITO/CdS isotype heterojunction.

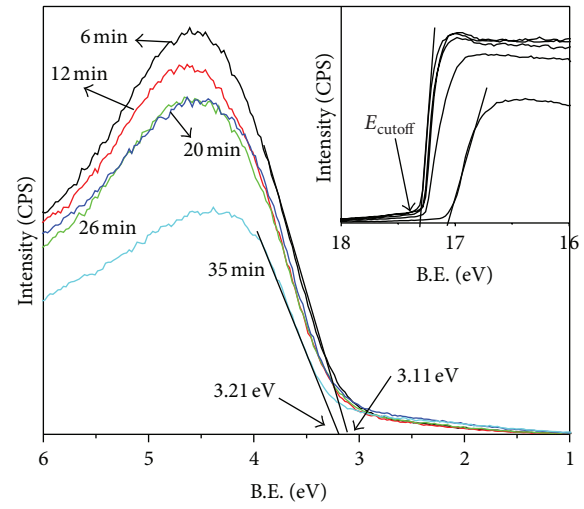

Figure 7: The UPS spectra of ITO/ZnO thin films.

The $h\nu$ is the excitation energy of Helium (21.2 eV), and the E_{Fermi} is set to be 0, so the Φ would be concluded to be 4.7 eV for CdS and 4.2 eV for ITO. And the interface dipole δ of ITO and CdS films can be obtained as 0.41 eV and 0.28 eV by

$$\delta = E_g - \text{VBM}. \tag{2}$$

The XPS at various times in Figure 5 shows the band energy variation at the interface of the ITO/CdS films. The profiling of samples starts CdS films and ends at 46 min, when the intensity peak of Cd3d is zero. The O1s emission gradually increases in intensity and the Cd3d decreases during the profiling process. At 1–9 min the intensity of O1s is weak and the B.E. is of no change because the content of oxygen atoms is very lower when the CdS films have been etched for 1 min. At 9–11 min, the intensity of O1s increases while the Cd3d decreases and the B.E. of Cd3d increases about 0.14 eV. That is to say, that the surface profiling occurs at 9–11 min. The thickness of CdS films is 150 nm, so the profiling speed is estimated as 15 nm/min. The intensity of Cd3d decreases gradually and passes off at 46 min. The results show a shift in all the core level lines to larger binding energies, which indicates the formation of a space charge layer (band bending) in the substrate.

In order to construct the band energy diagram, the position of E_F within the bulk must be known. The difference between the vacuum level ΔE_{vac} can be obtained by subtracting the overall band bending from the difference of the work functions by (x is electron affinity)

$$\Delta E_{\text{vac}} = (\chi_2 + \delta_2) - (\chi_1 + \delta_1) = 0.56\,\text{eV}. \tag{3}$$

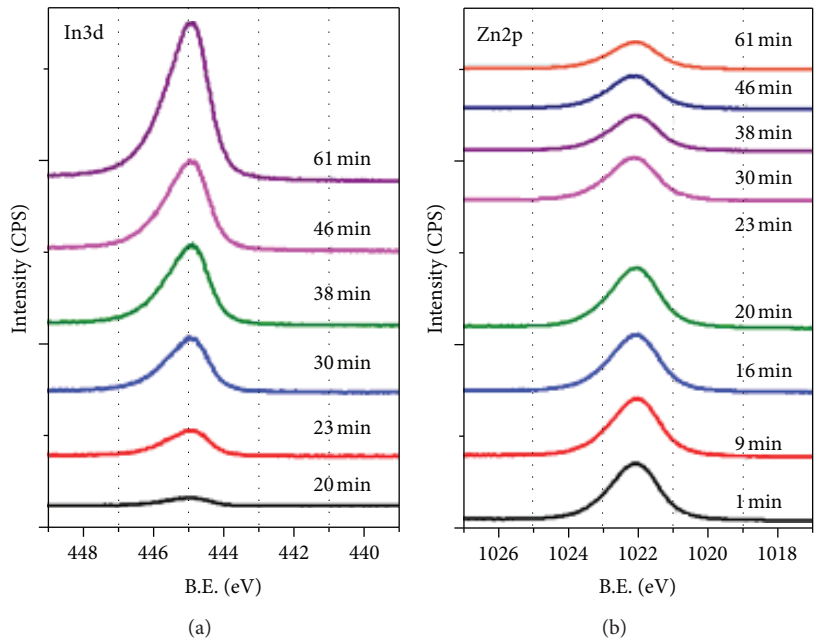

Figure 8: XPS spectrum in the In3d and Zn2p reigns for n-ITO/n-ZnO isotype heterojunction under various profiling time.

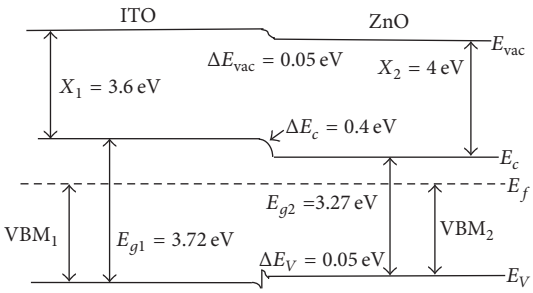

Figure 9: Energy band diagram of the ITO/ZnO isotype heterojunction.

Then the valence band offset ΔE_V can be determined by using the band energy difference between the O1s and Cd3d at intermediate coverage and the binding energies of the core levels with respect to the valence band. One has

$$\Delta E_V = (\mathrm{VBM}_1 - \mathrm{VBM}_2) - \Delta E_{\mathrm{vac}} = 0.61\,\mathrm{eV}. \quad (4)$$

Using the ΔE_V and the band gaps given before, the conduction band offset ΔE_c was calculated to be

$$\Delta E_c = \Delta E_{\mathrm{vac}} + (\delta_1 - \delta_2) = 0.9\,\mathrm{eV}. \quad (5)$$

Having determined band bending, band offset, and interface dipole, the final band alignment at the interface ITO/CdS heterojunction is presented in Figure 6. The conduction band bends upward in the ITO layer at the surface while the CdS layer bends downward. The electrons need to overcome a huge energy barrier (about 0.9 eV) when transferring from the CdS to ITO films.

3.3.2. ITO/ZnO System. The characterization of the layer at different profiling times is illustrated in Figure 7. The VBM increases from 3.11 eV to 3.21 eV at the interface of the ITO/ZnO films. And the Φ would be calculated to be 3.8 eV for ZnO and 4.1 eV for ITO. And the interface dipole δ of ITO and ZnO fims can be obtained as 0.51 eV and 0.16 eV.

The XPS at various profiling times in Figure 8 shows the variations in the band energy of the ITO/ZnO films at the interface (20–23 min). The profiling of samples starts ZnO films and ends at 61 min. The In3d (ITO) emission gradually increases in intensity and the Zn2p (ZnO) intensity decreases along the profiling progress. The thickness of ZnO films is 150 nm, so the profiling speed is estimated as 7 nm/min, which is obviously lower than CdS. And $\Delta E_{\mathrm{vac}} = 0.05$ eV was obtained and the valence band offset ΔE_V and conduction band offset ΔE_c were calculated to be 0.4 eV and 0.05 eV, respectively.

The final band alignment at the interface ITO/ZnO heterojunction is presented in Figure 9. The conduction band bends downward in the ITO layer while ZnO layer bends upward at the interface. The barrier energy is about 0.4 eV, which is lower than ITO/CdS heterojunction potential barrier. That is to say the introducing ZnO film is beneficial for the transfer and collection of electrons.

3.3.3. ITO/SnO_2 System. The interface profiling from 9 to 20 min is presented in Figure 10. At the interface of ITO/SnO_2, the VBM value decreases from 3.38 eV to 3.28 eV. The Φ of SnO_2 films would be calculated to be 4.14 eV and 4.06 eV for ITO films. And the interface dipole δ of ITO and SnO_2 films can be obtained as 0.44 eV and 0.73 eV.

The XPS at various profiling times is showed in Figure 11. The profiling of samples starts SnO_2 films and ends at 42 min, when the intensity of Sn3d passes off. It confirms that the In3d (ITO) emission increases in intensity and the Sn3d

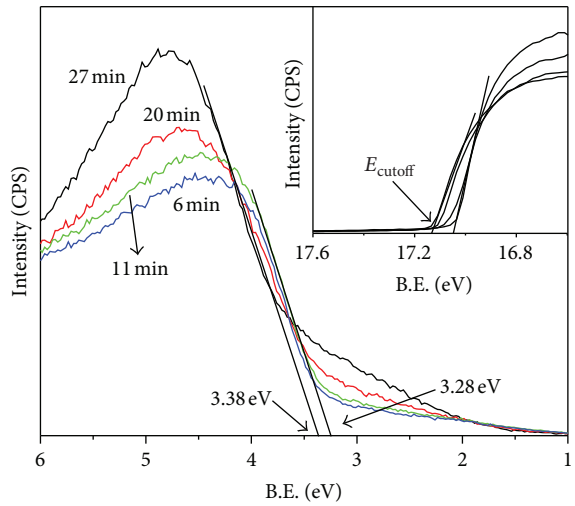

Figure 10: The UPS spectra of ITO/SnO_2 complex layers.

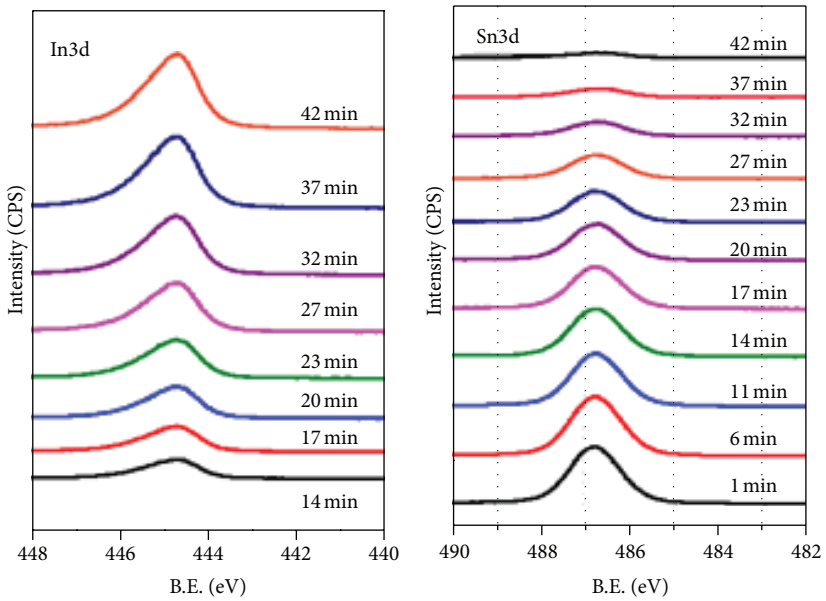

Figure 11: XPS spectrum in the In3d and Sn3d regions of an n-ITO/n-SnO_2 isotype heterojunction at various profiling times.

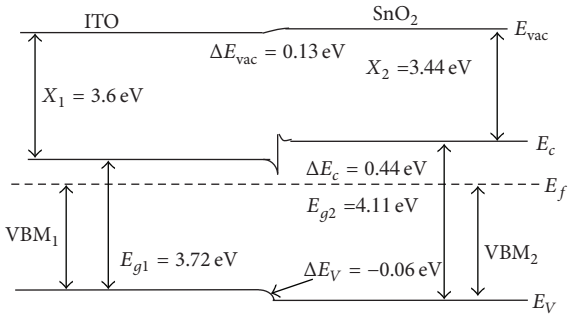

Figure 12: Energy band diagram of the ITO/SnO_2 isotype heterojunction.

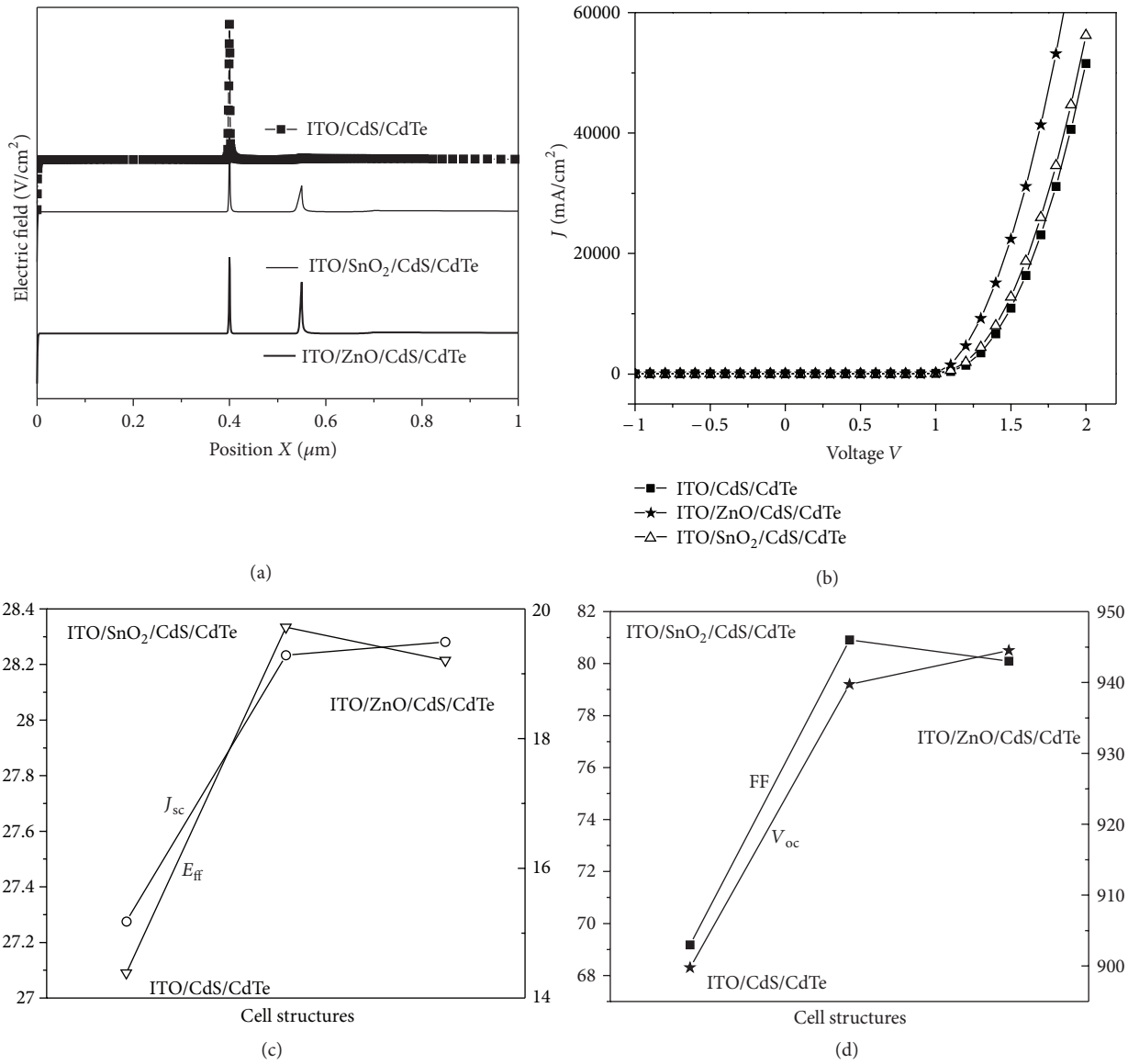

FIGURE 13: The simulated output performance for different structure: the electric field distribution (a), the dark IV curve (b), J_{sc} and E_{ff}, (c) and FF & V_{oc} (d).

(SnO_2) decreases during the profiling process. At 20–23 min, the profiling came to the interface, and the profiling speed is estimated as 7 nm/min and the thickness of SnO_2 film is 150 nm. The adding of SnO_2 films between ITO and CdS films also changes the energy structure. The ΔE_{vac} = 0.13 eV, ΔE_C = 0.44 eV, and ΔE_V = −0.06 eV were also obtained.

The energy band diagram is presented in Figure 12. The conduction band bends downward in the ITO layer at the surface while SnO_2 layer bends upward. The results shows that electrons must overcome an energy barrier (0.44 eV) when transferring from the SnO_2 to ITO films, which is also less than that in the ITO/CdS heterojunction. Thus adding SnO_2 layer is also beneficial for the transfer and collection of electrons.

3.4. Device Simulation. Based on the previous analysis, we have simulated the effect of ITO/ZnO and ITO/SnO_2 films in CdTe cells by AMPS-1D. Figure 13 shows the electric fields, dark I-V curves, and simulated output performance of different cells. The results show that inserting of ZnO or SnO_2 films changes the electric field distribution, with the electric field strength decreasing at the ITO/CdS interface and a new electric field appearing at the ZnO (or SnO_2)/CdS interface. These electric field distributions are beneficial for the transfer and collection of electrons in CdTe cells. The introduction of ITO/ZnO or ITO/SnO_2 films in CdTe solar cells improves the efficiency (E_{ff}), open voltage (V_{oc}), and short circuit current (I_{sc}) significantly.

Also, we fabricated CdTe solar cells with or without HRT films. The cells with ZnO films have the efficiency of 12.17%

(V_{oc} = 742 mV, J_{sc} = 26 mA/cm^2, FF = 62.6%, and area = 0.5 cm^2) and the sample with SnO_2 films has the efficiency of 11.4% (V_{oc} = 724 mV, J_{sc} = 25.8 mA/cm^2, FF = 61.2%, and area = 0.5 cm^2), while the sample without HRT layers has a much lower efficiency of 8.7% (V_{oc} = 689 mV, J_{sc} = 23.55 mA/cm^2, FF = 53.6%, and area = 0.5cm^2). The results also show that the introduction of HRT layers decreases the series resistance, which was partly attributed to good interface properties between HRT and CdS layers.

4. Conclusion

The ITO/ZnO and ITO/SnO_2 films were successfully deposited on a glass substrate by DC- and RF-magnetron sputtering. The optical transmittance of the ITO/ZnO and ITO/SnO_2 as complex TCO layers was 82% and 81.64% from 500 nm–850 nm, respectively. The measured sheet resistances of ITO/ZnO and ITO/SnO_2 layers were 10^5 Ω/□ and 37.5 Ω/□, respectively. The interface compositions of the TCO layers were characterized by UPS and XPS, and the energy band diagrams were determined. The energy barriers at the interface of ITO/ZnO and ITO/SnO_2 layers are almost 0.4 and 0.44 eV, which are lower than those at ITO/CdS heterojunctions (0.9 eV). The ITO/ZnO and ITO/SnO_2 as complex transparent conductive benefit the transfer and collection of electrons in CdTe solar cells and reduce the minority carriers recombination at the interface, compared to CdS/ITO.

Furthermore, we have also simulated and analyzed the effects of the ITO/ZnO and ITO/SnO_2 films on CdTe cells by AMPS-1D. The results show that the electric field distribution changes a lot by the introduction of ZnO and SnO_2 films between ITO and CdS. The E_{ff}, FF, V_{oc}, and I_{sc} are improved significantly, that is to say, the ITO/ZnO and ITO/SnO_2 complex transparent conductive layers are beneficial for the performance of CdTe solar cells.

Acknowledgments

This research was supported by the National Basic Research Program (973 Program) of China under Grant no. 2011 CBA00708.

References

[1] J. Herrero, M. T. Gutiérrez, C. Guillén et al., "Photovoltaic windows by chemical bath deposition," *Thin Solid Films*, vol. 361-362, pp. 28–33, 2000.

[2] K. L. Chopra, P. D. Paulson, and V. Dutta, "Thin-film solar cells: an overview," *Progress in Photovoltaics*, vol. 12, no. 2-3, pp. 69–92, 2004.

[3] Z. Fang, X. C. Wang, H. C. Wu, and C. Z. Zhao, "Achievements and challenges of CdS/CdTe solar cells," *International Journal of Photoenergy*, vol. 2011, Article ID 297350, 8 pages, 2011.

[4] X. Wu, "High-efficiency polycrystalline CdTe thin-film solar cells," *Solar Energy*, vol. 77, no. 6, pp. 803–814, 2004.

[5] C. S. Ferekides, D. Marinskiy, V. Viswanathan et al., "High efficiency CSS CdTe solar cells," *Thin Solid Films*, vol. 361, pp. 520–526, 2000.

[6] T. Minami, "Present status of transparent conducting oxide thin-film development for Indium-Tin-Oxide (ITO) substitutes," *Thin Solid Films*, vol. 516, no. 17, pp. 5822–5828, 2008.

[7] X. Wu, J. Keane, R. Dhere et al., "16.5%-efficient CdS/CdTe Polycrystalline thin film solar cell," in *Proceedings of the 17th European Photovoltaic Solar Energy Conference*, pp. 995–1000, Germany, 2001.

[8] C. S. Ferekides, R. Mamazza, U. Balasubramanian, and D. L. Morel, "Transparent conductors and buffer layers for CdTe solar cells," *Thin Solid Films*, vol. 480-481, pp. 224–229, 2005.

[9] S. Sheng, H. Hao, H. Diao et al., "XPS depth profiling study of n/TCO interfaces for p-i-n amorphous silicon solar cells," *Applied Surface Science*, vol. 253, no. 3, pp. 1677–1682, 2006.

[10] G. Liu, T. Schulmeyer, J. Brötz, A. Klein, and W. Jaegermann, "Interface properties and band alignment of Cu_2S/CdS thin film solar cells," *Thin Solid Films*, vol. 431-432, pp. 477–482, 2003.

[11] K. Horn, "Photoemission studies of barrier heights in metal-semiconductor interfaces and heterojunctions," *Applied Surface Science*, vol. 166, no. 1, pp. 1–11, 2000.

[12] J. C. Bernède and S. Marsillac, "Band alignment at the interface of a SnO_2/γ-In_2Se_3 heterojunction," *Materials Research Bulletin*, vol. 32, no. 9, pp. 1193–1200, 1997.

[13] W. Mönch, "Electronic properties and chemical interactions at III-V compound semiconductor surfaces: germanium and oxygen on GaAs(110) and InP(110) cleaved surfaces," *Applied Surface Science*, vol. 22-23, no. 2, pp. 705–723, 1985.

[14] A. Bouloufa, K. Djessas, and A. Zegadi, "Numerical simulation of $CuIn_xGa_{1-x}Se_2$ solar cells by AMPS-1D," *Thin Solid Films*, vol. 515, no. 15, pp. 6285–6287, 2007.

[15] M. A. Matin, M. Mannir Aliyu, A. H. Quadery, and N. Amin, "Prospects of novel front and back contacts for high efficiency cadmium telluride thin film solar cells from numerical analysis," *Solar Energy Materials and Solar Cells*, vol. 94, no. 9, pp. 1496–1500, 2010.

[16] M. A. Contreras, M. J. Romero, B. To et al., "Optimization of CBD CdS process in high-efficiency Cu(In,Ga)Se_2-based solar cells," *Thin Solid Films*, vol. 403-404, pp. 204–211, 2002.

[17] S. J. Fonash, *Solar Cell Device Physics*, Academic Press, New York, NY, USA, 1981.